MTech (Structural Engineering)

Rishabh Jain

2026

Experimental Study on the effect of Wind Pressure Disrubution on a Curved Shape Structure

A Dissertation Submitted
in Partial Fulfillment of the Requirement for the Award of
the Degree of

MASTER OF TECHNOLOGY

in

Structural Engineering

by

Rishabh Jain

(2K23/STE/505)

Under the supervision of

Dr. Ritu Raj, Professor

DEPARTMENT OF CIVIL ENGINEERING
DELHI TECHNOLOGICAL UNIVERSITY
(Formerly Delhi College of Engineering) Bawana Road, Delhi- 110042

May, 2026

DELHI TECHNOLOGICAL UNIVERSITY
(Formerly Delhi College of Engineering)
Bawana Road, Delhi-110042

CANDIDATE DECLARATION

I, **Rishabh Jain**, M. Tech (Structural Engineering) student, having **Roll no: 2K23/STE/505**, hereby certify that the work which is being presented in the dissertation entitled "**Experimental Study on the effect of wind pressure distribution on Curved Shape Structure**" in the partial fulfilment of the requirements of the award of the Degree **Master of Technology in Structural Engineering**, submitted in the **Department of Civil Engineering, Delhi Technological University** is an authentic record of my work carried out under the supervision of Prof. Ritu Raj, Department of Civil Engineering, Delhi Technological University, Delhi. The matter present in this dissertation has not been submitted by me for the award of any other degree of this or any other institute.

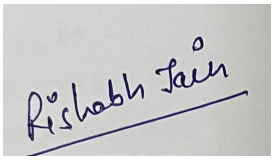

RISHABH JAIN
(2K23/STE/505)

DELHI TECHNOLOGICAL UNIVERSITY
(Formerly Delhi College of Engineering)
Bawana Road, Delhi-110042

CERTIFICATE

I hereby certify that the project Dissertation entitled "**Experimental Study on the effect of wind pressure distribution on a Curved Shape Structure"** which is submitted by Rishabh Jain, Roll No. 2K23/STE/505, to Department of Civil Engineering, Delhi Technological University in partial fulfillment of the requirement for the award of the degree of Master of Technology, is a record of project work carried out by her under my supervision. To the best of my knowledge this work has not been submitted in part or full for any Degree or Diploma to this University or elsewhere.

DR. RITU RAJ
(Professor and Supervisor)
Department of Civil Engineering

ABSTRACT

The present study deals with the distribution of wind pressure on the curved-shaped high-rise structure by means of wind tunnel testing system. A very stiff scale model of building was placed in a wind tunnel and subjected to simulated atmospheric boundary layer conditions for a variety of wind directions and reference wind speeds. Pressure measurements were performed utilizing an array of pressure taps located on the windward, leeward and side façades.

The gathered data were processed to determine the fluctuating pressure coefficients, which permitted a detailed evaluation of the aerodynamic performance. The effect of curvature on flow separation, wake creation and localized high suction zones was studied and compared to typical rectangular building forms. The results show that the use of curved geometry can lead to a reduction of the total aerodynamic drag, but at the same time causes high local negative pressures and pressure fluctuations. The results emphasize the significance of precise wind load assessment for the safe design of façade and structural members of curved high-rise shaped buildings.

ACKNOWLEDGEMENT

I, **RISHABH JAIN**, would like to offer a special thanks to all those who have contributed to the successful completion of this thesis.

I express my deepest gratitude to my supervisor Prof. Dr. Ritu Raj, Delhi Technological University. He introduced me to the world of research from scratch, my time with him also has helped me to grow in many ways. His comments at every stage of my writing and instances on perfection have helped this It is not only careful supervision but also his personal affection that has given me lot of confidence to proceed smoothly with my work. Words cannot express my gratitude to my supervisor for patiently helping me to think clearly and consistently by discussing every point of this dissertation with me. It is my privilege to work with him in my post-graduation.

I am grateful to the faculty and staff of Delhi Technological University [DTU], especially the Civil Engineering Department, for providing a conducive academic environment and necessary resources for carrying out this research. The access to the laboratory facilities and library resources has greatly facilitated the experimental work and literature review.

I am also thankful to **Prof. Awadhesh Kumar,** Head of the Department of Civil Engineering, Delhi Technological University, Delhi, for giving me this opportunity to do this work and to all the staff members of the Department of Civil Engineering for their constant encouragement.

I would also like to extend my sincere thanks to all the faculty members, laboratory staff, and research scholars of the department for their technical support, insights, and cooperation during the simulation and experimental phases of this project

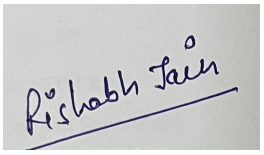

RISHABH JAIN

2K23/STE/505

CONTENTS

CANDIDATE DECLARATION **2**

CERTIFICATE 3

ABSTRACT **4**

ACKNOWLEDGEMENT **5**

CONTENTS **6**

LIST OF TABLES **9**

LIST OF FIGURES **9**

CHAPTER 1 ..... **10**

INTRODUCTION **10**

1.1 Wind Tunnel 10

1.2 Classification of Wind Tunnel 11

1.3 Classification is done based upon the Speed and Mach No: 11

1.3.1 Mach Number: 11

1.4 Mode of operation is classified as: 12

1.5 Classification according to type of test: 14

1.6 Advantages of closed loop wind tunnel upon open loop wind tunnels: 15

1.7 Components of Closed-Loop Wind Tunnels 15

1.7.1. Settling Chamber and Flow Straightener 15

CHAPTER 2 ..... **18**

LITERATURE REVIEW **18**

2.1 General 18

2.2 Research Gaps 19

CHAPTER 3 ..... **20**

METHODOLOGY..... 20

3.1 Principle of Operation.....20

3.2 Measurements using wind tunnels:.....20

3.3 Pressure measurements:.....20

3.4 Force & Moment measurements:.....21

3.1 Applications of Wind Tunnels :.....21

3.2 Aerodynamics applications:.....21

3.3 Non Aerospace and Industrial Applications:.....22

3.4 Computational Fluid Dynamics CFD.....22

3.5 Governing Equation.....22

3.6 Working Principle of CFD Codes.....25

3.7 Pre-Processing.....25

3.8 Solver Architecture.....26

3.9 Post-Processing.....27

3.10 Advantages and Disadvantages.....27

3.11 Applications of CFD.....28

3.12 Turbulence Modeling and Viscosity Prediction.....28

3.13 k-ε Model Framework.....28

3.14 Exact Transport Equation for Turbulent Kinetic Energy (k).....29

3.15 Viscous Dissipation Rate.....30

3.16 Turbulent dissipation (k -E):.....30

CHAPTER 4..... 32

EXPERIMENTAL WORK..... 32

4.1 Analytical Flow Computations (Input Conditions).....32

4.2 Ansys Workbench Simulation.....33

4.3 Recorded Data.....35

At Face A (0^0) 38

At Face A (30^0) 38
At Face A (60^0) 38
At Face A (90^0) 39
At Face A (120^0) 39
At Face A (150^0) 39
At Face A (180^0) 40
At Face B (0^0) 40
At Face B (30^0) 40
At Face B (60^0) 41
At Face B (90^0) 41
At Face B (120^0) 41
At Face B (150^0) 42
At Face B (180^0) 42
At Face C (0^0) 42
At Face C (30^0) 43
At Face C (60^0) 43
At Face C (90^0) 43
At Face C (120^0) 44
At Face C (150^0) 44
At Face C (180^0) 44
CHAPTER 5 45
RESULTS AND DISCUSSIONS 45
CHAPTER 6 47
CONCLUSION 47
REFERENCES 48
PLAGIARISM REPORT 50

LIST OF TABLES

Table 1: Mach Speed 11

LIST OF FIGURES

Figure 1: **Pressure Storage type wind tunnel.** 13
Figure 2: **A pressure vacuum wind tunnel** 13
Figure 3: **Open loop wind tunnel** 14
Figure 4: **Closed loop wind tunnel** 14
Figure 5: **Typical lift coefficient (CL) versus angle of attack (α) curve** 21
Figure 6: **Flow Diagram** 26
Figure 7: Ansys Dialogue Box 33
Figure 8: Model Plan View 36
Figure 9: Model Elevation View 37
Figure 10:A (At 0^0) 38
Figure 11: A (At 30^0) 38
Figure 12-**A (At 60^0)** 38
Figure 13-**A (At 90^0)** 39
Figure 14: -**A (At 120^0)** 39
Figure 15:-**A (At 150^0)** 39
Figure 16: -**A (At 180^0)** 40
Figure 17: -**B (At 0^0)** 40
Figure 18: -**B (At 30^0)** 40
Figure 19: -**B (At 60^0)** 41
Figure 20: -B (At 90^0) 41
Figure 21: -B (At 120^0) 41
Figure 22: -**B (At 150^0)** 42
Figure 23: -B (At 180^0) 42
Figure 24: -C (At 0^0) 42
Figure 25: -C (At 30^0) 43
Figure 26: -**C (At 60^0)** 43
Figure 27: -**C (At 90^0)** 43
Figure 28: -C (At 120^0) 44
Figure 29:-C (At 150^0) 44
Figure 30:-C (At 180^0) 44

CHAPTER 1

INTRODUCTION

1.1 Wind Tunnel

Wind tunnels having big tubes that move air through them. High rise structures built to mimic the aerodynamic properties of an aircraft or object in flight. Scientists use wind tunnels to study the flight characteristics of an aeroplane. Full scale vehicles can be tested in some large wind tunnels. The facilities recreate the circumstances of flying by blowing air over the vehicle while it is held still.

Usually, high-powered fans are used to push air down the tunnel. The specimen is fixed in the tunnel so that no movement takes place during the test. The object may be a miniature model of a car. In such cases the subject may be only a certain section of the vehicle. The test can be performed for the full aircraft & spaceship. This test does not require to execute a highly complex task it is simple such as rotating the fan blade. The air is blowing around a stationary object it shows that the thing will exert a force which will try spin with the help of air. Flow of air can be studied in various ways. Smoke & Coloured powder, emitted directly into the atmosphere and visible to the naked eye as they fly. There are various unique types of instruments which can be utilized and threads attached to it and it indicates the direction of blowing air. Special sort of devices are used routinely to measure the air pressure on the specimen.

Wind Tunnels Technology was developed after the Aeroplan was developed massive wind tunnel were built in World War II and were needed to save the fighter plane. During the Cold War period the evolution of new & specialized technology was used for the evolution of supersonic aircraft and weapons. Proper planning becomes more crucial and at this moment wind tunnel testing needs to be highly in demand.

The advancement technology of CFD modelling for high-speed digital computers has been applied to minimize wind tunnel demand.
However, results of Computational Fluid Dynamics (CFD) are not always correct and wind tunnel testing is required to validate the CFD results.

1.2 Classification of Wind Tunnel

Wind tunnels can also be categorized in the various types:

Speed and Mach no:

It can be classified as low-speed or high-speed wind tunnels. A high speed wind tunnel, which operates at a speed where compressibility effects are important in wind tunnel jargon. It is also classified according to the operational Mach number in wind tunnel as subsonic wind tunnel, transonic wind tunnel, supersonic wind tunnel and hypersonic wind tunnel.

Method of operations are (1)Pressure storage, (2) in-draft & (3) Pressure vacuum type.

Type of test section (TS) — Open, Closed or Semi-enclosed

1.3 Classification is done based upon the Speed and Mach No:

1.3.1 Mach Number:

"Mach number is ratio of speed of sound and speed of flow after some critical point".

In layman's terms it is ratio of velocity of body to velocity of sound in the medium of which it is a part.

mach Number (m = u/c)

where, m = Mach number u = local flow velocity (m/s), v = sound speed in that medium (m/s)

If object speed lesser than speed of sound, it said to be in the subsonic state & if speed object is greater than speed of sound, it said to be in the supersonic state. These terms are used by scientists practically aerodynamics effect most of time to describe a range of mach values.

Table 1: Mach Speed

Type of Flow	Sub-sonic	Tran-sonic	Sonic	Super-sonic	Hyper-sonic	High Hypersonic
Mach No.	<0.8	0.8-1.3	1.0	1.3-5	5-10	>10

- **Subsonic:** Mach number strictly less than 0.8. Airflow across all portions of the vehicle is still well below the speed of sound.
- **Transonic:** The Mach value is in the range 0.8-1.3. In this regime there are pockets of subsonic and supersonic flow simultaneously across different areas of the aircraft. Aircraft flying here often have sweeping wings designed to delay wave drag.
- **Sonic:** Mach number is exactly 1.0, therefore the velocity is equal to local speed of sound
- **Supersonic:** Mach levels are in the range of 1.3 – 5.0. The flow over the whole vehicle is fully supersonic. Supersonic aircraft have different structural characteristics. They have all-moving canards/stabilators, sleek aerofoil sections, and sharp leading edges.
- **Hypersonic:** Mach numbers between 5.0 and 10. These are very specialised aircraft, with such things as actively cooled nickel-titanium skins and narrow, sweeping wings to cope with severe aerodynamic heating. For example, U.S. X-15 aircraft set a world record by flying Mach.
- **High-Hypersonic:** Mach levels vary from 10 till 25. At these high velocities thermal protection systems become the major design consideration because of severe aerodynamic heating and analysis of surface temperatures becomes crucial.

1.4 Mode of operation is classified as:

•Pressure storage type:

Intermittent blow down tunnel: In one of these tunnels air expands from a high pressure to low pressure chamber. Otherwise, the ambient air can be stretched down at a very low vacuum (intermittent indraft wind tunnel).

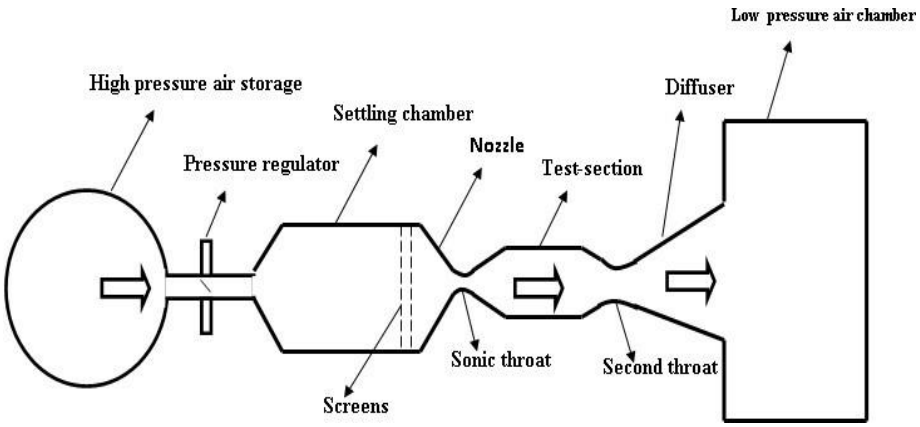

Figure 1: **Type of Pressure Storage wind tunnel.**

- **Pressure vacuum type :**

Open return tunnels is a wind tunnel at both end and sucks the air from room to the text part. A blow down air in wind tunnel is a high-pressure upstream of test section and a low pressure reservoir downstream of test section

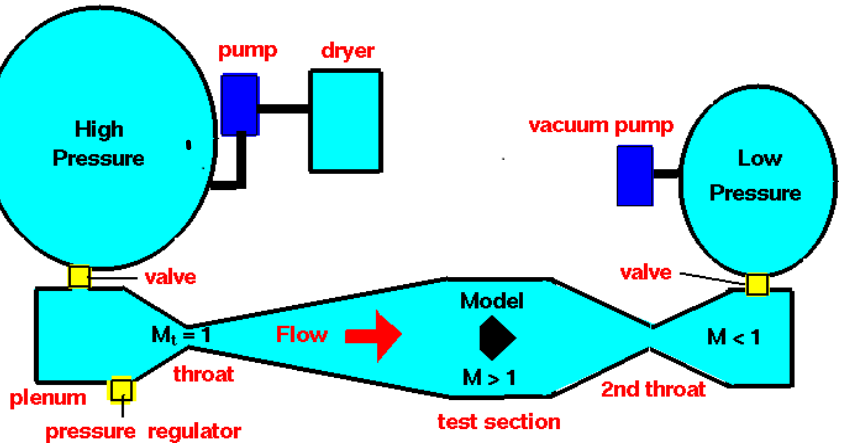

Figure 2: **A pressure vacuum wind tunnel**

1.5 Classification according to type of test:

- Open loop Wind Tunnel

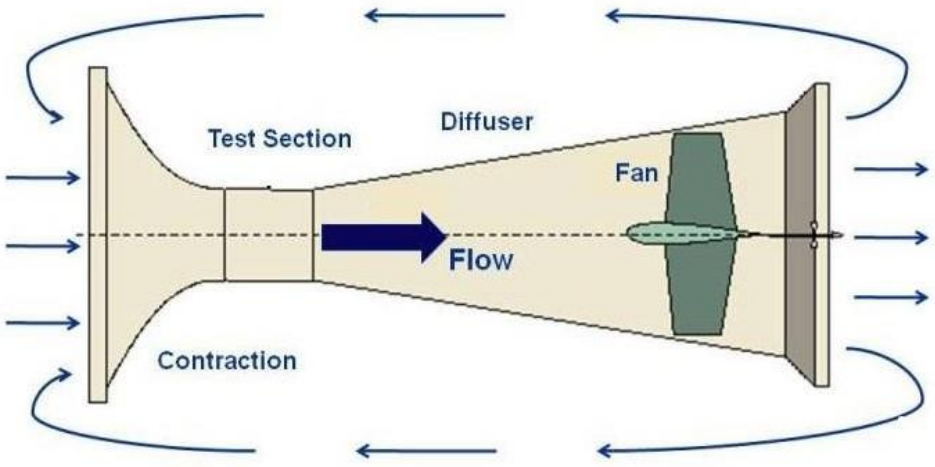

Figure 3: Open loop wind tunnel

In open section of tunnel, air flowing through test section is taken from room in which tunnel showing arrows in figure represent movement of air in wind tunnel inside room.

- Closed Loop Wind Tunnel

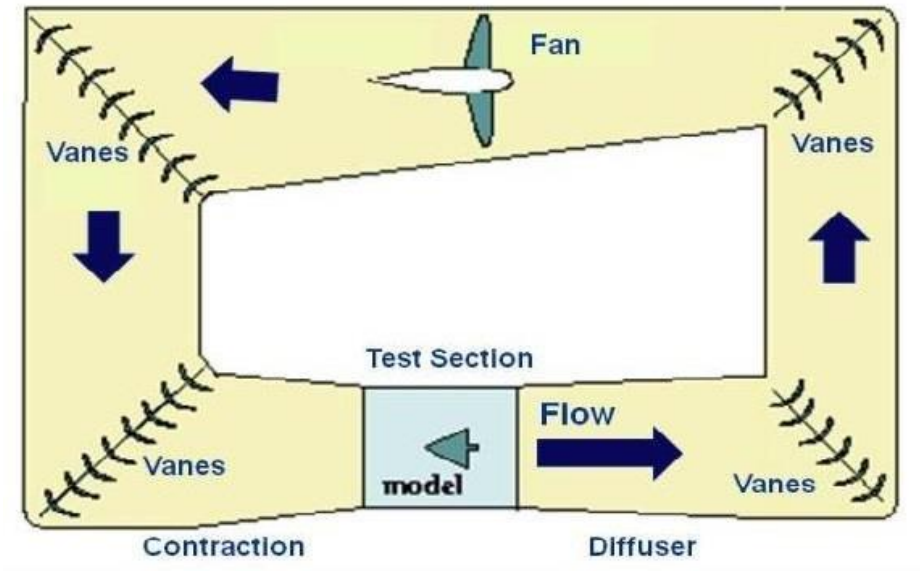

Figure 4: Closed loop wind tunnel

A closed back tunnels the air blows through a series of revolving vanes to return to the fan. After passing out fan, air is returned to contraction section and return to test section. Closed return tunnel duct construction is continuously ventilated with the air. Arrows shown in figure indicate passage of air through wind tunnel.

Closed returns may have subsonic or supersonic tunnels. Besides, the supersonic closed return tunnels is more difficult than the subsonic tunnel. Low pressure inside test section can promote the formation of condensation in the test section and this is generally avoided by drying the air that enters the test section through a drier bed . Usually there is an extra throat downstream of the test portion in the tunnel shock down supersonic flow to subsonic.

1.6 Advantages of closed loop wind tunnel upon open loop wind tunnels:

The force needed to achieve particular speed is reduced.

- Matter can be stored within the circuit.
- The noise & vibration mitigation level is much quieter.
- Air entering test section should be free of dust particle.
- Fan blades are not as more dangerous to harm the model failure.

1.7 Components of Closed-Loop Wind Tunnels

1.7.1. Settling Chamber and Flow Straightener

The settling chamber is usually a combination of honeycombs and wire mesh screens. It is mostly used to reduce turbulence severity to guide the incoming flow only in the axial direction. air may enter the settling chamber from different angles; in downstream parts only uniform, axial flow is permissible.

Screens typically attenuate the spatial changes of the velocity and fragment larger turbulent eddies into smaller, more rapidly decaying ones. However, they are also important as a debris barrier. The honeycomb structure comprises of cells of different geometries (usually hexagonal) that are orientated parallel to the freestream direction. The honeycomb is designed with a high L/D ratio to minimise cross flow with a small streamwise pressure decrease.

1.7.2. Contraction Section (Nozzle)

Contraction section is designed to accelerate the low-speed flow leaving settling chamber to feed it test section at the required velocity. This local acceleration causes a large decrease of the relative cross-sectional velocity fluctuations and thereby improves the flow homogeneity.

Geometrically, a modest radius of curvature is generally used at the inlet, which increases linearly to a higher radius of curvature at the exit where it connects to test section. The wall profile must be designed carefully to avoid boundary-layer separation at the intake due to adverse pressure gradients and to avoid flow unsteadiness at the exit. The contraction section length is limited to a minimum to reduce boundary-layer growth and maximise the contraction area ratio.

1.7.3 Test Section

In this test section is core of wind tunnel method and dictates design of all other elements. This part is supplied with aerodynamic models. They are exposed to the appropriate freestream velocity. Test sections are manufactured with different cross-section forms, e.g. rectangular, hexagonal or octagonal, depending on usefulness, cost of manufacture and aerodynamic factors.

The length of the test section is normally set be 1 to 2 times its principal cross-sectional size. It shall have enough optical access (windows) and instrumentation ports for testing requirements. Flow quality in an ideal test section is characterised by a constant, uniform velocity profile at the intake, little cross-flow, low turbulence intensity, and small boundary-layer growth along the walls.

1.7.4. Diffuser

Immediately downstream of the test section there is a diverging duct with gradually increasing cross section area, i.e. the diffuser. Its role is to slowly decrease the flow velocity, and thereby recover the kinetic energy as static pressure (pressure recovery).

The diffuser is a very important part in design of the wind tunnel. Maximising static pressure recovery minimises the overall pressure losses in the circuit, reducing the fan power demand (which scales with the cube of the test section velocity). Traditionally, the overall divergence angle (cone angle) of the diffuser limited to 70 or less to avoid flow reversal and catastrophic boundary-layer separation.

1.7.5. Turning Vane

The air in closed-circuit wind tunnel must go around four 900 corners to flow back on itself. Aerodynamic turning vanes are fitted at the corners of these bends to avoid massive flow separation and turbulence and pressure losses at these bends.

These vanes consist of highly cambered structural airfoils or curved plates that efficiently guide the fluid around the corners. In high performance installations these vanes are made movable to fine tune the flow direction, eliminating under-turning or over-turning of the air stream and assuring extremely symmetric flow when it returns to the settling chamber.

CHAPTER 2

LITERATURE REVIEW

2.1 General

In modern aerodynamics and wind engineering the combination of Computational Fluid Dynamics (CFD) with experimental fluid mechanics has revolutionised the design process. In the past, numerical models were used to assess only isolated flow components, for example, test sections or individual printed circuit board (PCB) cooling channels (Launder and Spalding, 1972; Ghani et al., 2001). However, the use of CFD can be optimise the full wind tunnel circuit configurations is still a field of active development (Moonen et al., 2006).

Full-Tunnel Circuit Modeling: Calautit (2014) verified thorough design process of a closed-loop subsonic wind tunnel. Analytical expressions were used to model the pressure losses directly as boundary conditions of the domain, mimicking the full-scale architecture and not an isolated test section. This entire circuit technique validated that internal guide vanes greatly improve free stream flow uniformity and lower structural power requirements.

Grid Independence and Error Reduction: Flow quality requirements were tested by Moonen et al. (2006; 2007) with steady state, 3D RANS simulations (K-ε Model). Through exhaustive grid sensitivity analysis, they showed that full circuit wind tunnel models boost the absolute prediction accuracy by a factor of 2 to 4 compared to legacy models that only use the test section. Their results also reveal that, while vertical guide vanes minimise lateral flow angularity and velocity skewness, horizontal profiles can induce localised parasitic wake losses if not properly aligned.

Flow Efficiency Optimization: Gordon and Imbabi (1998) used CFD downscale physical and capital footprint of the University of Aberdeen closed-loop wind tunnel without imposing flow separation. Meanwhile, micro-heat exchanger investigations (Harris et al., 2000; Bhutta et al., 2012) have demonstrated that commercial CFD tools employing pressure-velocity coupling schemes (e.g. SIMPLE, PISO) are able to accurately predict pressure drops, fluid maldistribution and thermal fields inside compact cross-flow heat exchangers.

2.2 Research Gaps

The gradual aerodynamic heating in standard closed-loop wind tunnels results from the constant viscous dissipation of the recirculating air. Traditional systems use individual heat exchangers with fixed fluid characteristics, resulting in large pressure drop (delta p) penalties.

In this study, a unique compact triangular closed loop wind tunnel geometry dual-function guide vane radiators presented. The design further reduces thermal accumulation by geometry-matching the interior turning vanes to serve as liquid-to-gas cooling surfaces, while minimising total circuit head losses.

CHAPTER 3

METHODOLOGY

3.1 Principle of Operation

The air is either forced or pulled through a duct with a see-through window and sophisticated instruments. Scale models or geometric shapes are installed in the duct for aerodynamic study. Usually, the air propelled by the tunnel of a succession of axial or centrifugal fans.

However, flow coming straight out of a fan is very turbulent and rotating because of the moving blades and is not good for accurate aerodynamic measurements. Air flowing through the test section must be of very consistent quality with very low turbulence intensity. To do this the flow is passed through closely spaced honeycombs, screens and turning vanes to remove swirl and damp down turbulent eddies before the test model. Also, a closed-loop wind tunnel, air is continuously recirculated. There will be frictional losses in the wind tunnel, converting kinetic energy to thermal energy and increasing the air temperature. The circuit needs integrated cooling devices such as water cooled heat exchangers to keep the fluid characteristics constant and to prevent errors due to thermal expansion.

3.2 Measurements using wind tunnels:

3.3 Pressure measurements:

Flush-mounted surface pressure taps coupled to transducers can be embedded in the surfaces of a model to monitor local static pressure distribution over the surfaces. While surface pressure integration is useful for assessing pressure-dominated processes (e.g., form drag and lift generation), it only includes normal pressures on the body and does not account for tangential skin-friction shear stresses.

3.4 Force & Moment measurements:

By mounting the model on an internal or external strain-gauge force balance, researchers can directly measure global aerodynamic forces (lift, drag, and side force) & moments (rolling, and pitching moments) upon a specified range of angles of attacks (α).
Data captured for plotting fundamental aerodynamic performance curves, such as the lift coefficient (C_L) versus angle of attack (α) curve explained in Fig.5.

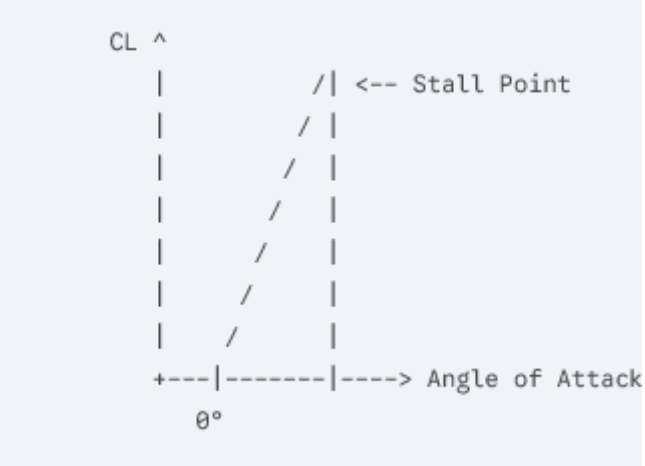

Figure 5: Typical lift coefficient (CL) versus angle of attack (α) curve

Note That: Physical struts and mounting structures of the force balance introduce aerodynamic interference, creating parasitic drag and localized turbulence that can compromise measurement accuracy. To minimize these experimental errors, supporting structures are meticulously streamlined or shielded using aerodynamic fairings.

3.1 Applications of Wind Tunnels :

3.2 Aerodynamics applications:

Wind tunnels offer a very well controlled uniform and quantifiable stream of fluid. They are commonly used in the aerospace and automotive industries to optimise vehicle designs, minimise drag, and refine overall stability. Besides industrial research, specialised vertical wind tunnels used for entertaining purpose serving as indoor, outdoor & skydiving attractions.

3.3 Non Aerospace and Industrial Applications:

While vehicle drag receives significant engineering attention due to its direct impact on fuel consumption and top-velocity thresholds, non-aerospace applications are vast:
Automotive Engineering: Evaluation of downforce (lift reduction) to ensure high-speed stability and cornering control for performance and racing vehicles.
Civil & Structural Engineering: Testing the wind-induced structural loads, vortex-shedding frequencies, and aeroelastic stability of skyscrapers, long-span bridges, and wind turbines.
Mechanical Engineering & Calibration: Fundamental fluid mechanics research, flow-visualization studies, and the precision calibration of anemometers and velocity probes.

3.4 Computational Fluid Dynamics CFD

Computational fluid dynamics (CFD) is a branch of fluid mechanics that uses numerical analysis and data structures to solve and analyse problems that involve fluid flow. The multi-physical interactions between fluids and gases and complicated engineering surfaces are simulated by means of millions of calculations, performed by high-performance computers.
Even with reduced transport equations and high-speed supercomputers, numerical solutions are only approximations to exact physical processes. Both in academia and in industry, the development of highly accurate and computationally efficient codes for the simulation of complicated situations, such as high-speed supersonic regimes or highly non-linear turbulent flows, is an active field of continuing research.

3.5 Governing Equation

In this equations for fluid flows are mathematically formulations of fundamental conservation of principle of physics each differential equations correspond directly to some physical conservation principle. The basic framework of fluid dynamics serving by 3 universal conservation laws: 1)Conservation of mass 2)Conservation of momentum, and 3)Conservation of energy.
Unsteady, Three-Dimensional Continuity Equation (Conservation of Mass):

$$\frac{\partial \rho}{\partial t} + \nabla \cdot (\rho \mathbf{u}) = 0$$

Alternatively, in divergence (div) vector notation:

$$\frac{\partial \rho}{\partial t} + \operatorname{div}(\rho \mathbf{u}) = 0$$

1. Momentum Equation (Conservation of Momentum - x-direction shown):

$$\frac{\partial(\rho u)}{\partial t} + \operatorname{div}(\rho u \mathbf{u}) = -\frac{\partial p}{\partial x} + \operatorname{div}(\mu \operatorname{grad} u) + S_{M_x}$$

Where, P represents static pressure, μ is dynamic viscosity, and S_{Mx} represents generalized body forces acting on the fluid element per unit volume.

2. Energy Equation (Conservation of Energy):

$$\frac{\partial(\rho i)}{\partial t} + \operatorname{div}(\rho i \mathbf{u}) = -p \operatorname{div}\mathbf{u} + \operatorname{div}(k \operatorname{grad} T) + \Phi + S_h$$

Where, i=internal energy; k=thermal conductivity; T=temperature; ϕ=viscous dissipation function, which accounts for irreversible conversion of kinetic energy to thermal energy; Sh=volumetric internal heat sources.

The continuous physical domain needs to be discretised into points or volumes to numerically solve the governing partial differential equations. Three main mathematical discretisation approaches are used in CFD architectures:

1. **Finite Difference Method (FDM):** Uses algebraic differences at localised grid nodes to approximate the derivatives in the governing equations. It is basic and of historical importance but mostly applies to geometrically structured meshes.

The discretisation of the Finite Difference Method (FDM) immediately obtained from differential form of partial differential equations (PDEs) to be solved. The derivatives appearing in governing equations are approximated algebraically with the help of using local Taylor series expansions.

The computational method is discretised into a grid of nodes (usually hexahedral or Cartesian blocks) and the discrete solution is computed explicitly at these nodal positions. FDM is mathematically simple and straightforward on structured Cartesian meshes, but it involves sophisticated curvilinear coordinate transformations to

translate onto geometries that cannot be easily represented by typical orthogonal elements.

2. **Finite Volume Method (FVM):** Utilizes the governing equations upon the discrete volume for each volume in the domain. This is the most common method used in commercial CFD codes, it ensures that the amounts are conserved through the cell faces.

The (FVM) discretises using integral version of serving transport equations computed a discrete control volume (cell). The continuous computational domain is discretised into a mesh of consecutive finite volumes. Governing equations are integrated over each individual volume, guaranteeing the conservation of fields over all cell faces by the computed fluxes.

The main advantage of FVM over FDM is its natural compatibility with fully unstructured grids, without the necessity for internal coordinate transformations on complex geometries. Traditionally, field variables are located in the geometric cell centers instead of the nodes. The values of the field variables at non-storage places such as at cell faces or element vertices are obtained by numerical interpolation algorithms.

3. **Finite Element Method (FEM):** Utilizes localized piece-wise continuous functions (shape functions) to approximate solutions across unstructured elements. It is mathematically robust and highly adaptable to complex boundary geometries, frequently used in (FSI) analysis.

The (FEM) discretisation based on a part-wise continuous representation of solution on local elements with prescribed mathematical basis (or form) functions. The world-wide domain is discretised into a number of unstructured geometric entities (finite elements).

The classical conservation equations are converted to their technically "weak form" by multiplying differential equations of appropriate test functions and integrating across element domain. FEM allows for a continuous analytical approximation of the solution field inside the elements, but requires sophisticated formulations of the boundary conditions and careful selection of basis functions to assure stability.

Parameter	Finite Difference Method (FDM)	Finite Volume Method (FVM)	Finite Element Method (FEM)
Mathematical Base	Differential form of PDEs	Integral form of PDEs	Weak form (Weighted residuals)
Grid Structure	Strictly structured / Curvilinear	Unstructured / Arbitrary polyhedra	Unstructured (Highly flexible)
Conservation	Conservative only if grid is orthogonal	Inherently conservative at cell level	Conserved globally, not locally
Variable Storage	At grid nodes	Cell centers (or face centers)	At Element Nodes

3.6 Working Principle of CFD Codes

Commercial CFD software are based on particular numerical techniques for dealing with fluid transport problems. These programs have a unique three-tier architecture to support problem definition and data extraction:

```
[Pre-Processing] ---> [Numerical Solver] ---> [Post-Processing]
```

3.7 Pre-Processing

This foundational phase involves converting the physical fluid problem into a structured digital format suitable for the numerical solver. The pre-processing pipeline includes:

Geometry Definition: Defining the physical boundaries of the fluid domain.

Grid/Mesh Generation: Subdividing the domain into non-overlapping elements or control volumes.

Physical Modeling: Selecting the fluid properties and specific equations to execute (e.g., laminar, turbulent, multiphase, thermal).

Boundary Conditions: Imposing fixed values or gradients (e.g., inlets, outlets, walls) on the boundary faces.

Note: Solution accuracy scales directly with mesh density, although finer meshes increase hardware memory usage and computation time significantly. Modern solvers circumvent this using automatic adaptive mesh refinement (AMR) in regions of

significant gradients

3.8 Solver Architecture

The numerical calculations are done by the solver. ANSYS develops industry standard products like FLUENT and CFX which use different discretisation algorithms. The solver uses a cell-vertex finite-element method with a coupled algebraic multigrid solver methodology. ANSYS FLUENT, on the other hand, employs a cell-centered finite volume method with segregated, density-based and coupled pressure-based solver approaches.

For pressure-based segregated solver loop (e.g. default SIMPLE method), the coupled non-linear governing equations are solved iteratively in the following order:

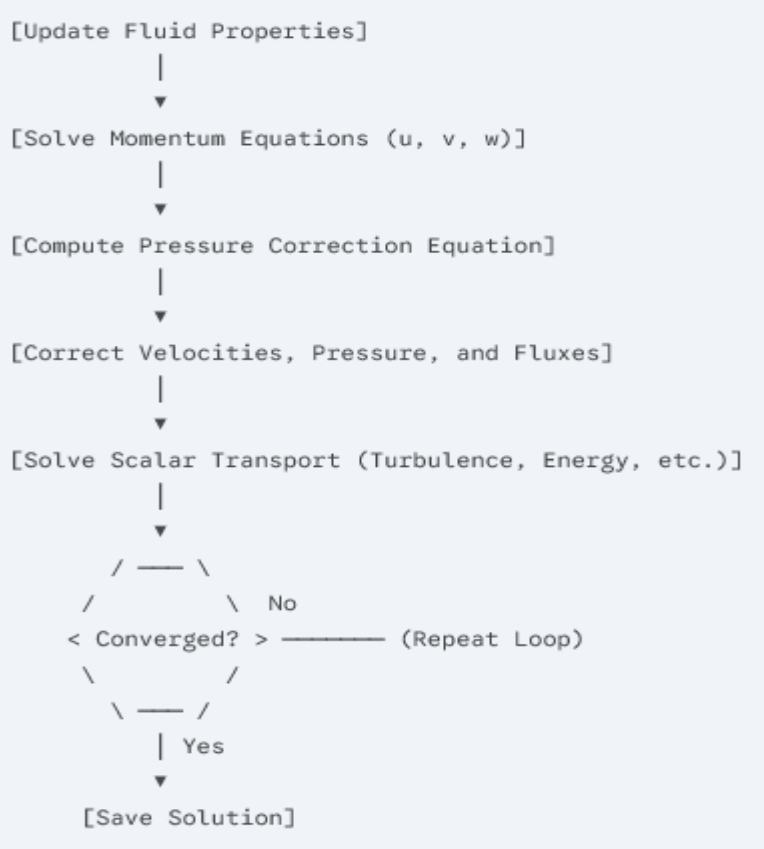

Figure 6: **Flow Diagram**

1. **Property Update:** Fluid properties (density, viscosity, thermal conductivity) are updated upon the current initialization.
2. **Momentum Solution:** The 3 momentum equations (x, y, z) are solved consecutively with the help of current pressure field to update the velocity vectors.
3. **Pressure-Velocity Coupling:** Since, New velocity fields are not always flow fields satisfying continuity equation, the pressure-correction equation constructed by combining the continuity equation with linearised momentum relations. This results in a corrected pressure and conservation of mass.
4. **Scalar Transport:** Additional transport equations for scalars including turbulent kinetic energy (k), dissipation (ε), chemical species, Energy—are solved sequentially.
5. **Convergence Check:** Residuals for all equations are compared with set convergence tolerances. Then loop repeats if criteria are not met.

The equations are linearised by an implicit technique in order to keep the numerical precision. Cell face spatial values are reconstructed from cell center storage nodes with a second order upwind interpolation algorithm. Pressure values are interpolated in the conventional way.

3.9 Post-Processing

The raw numerical matrix data are post-processed, organised, visualised and analysed. Modern post-processing tools (like ANSYS CFD-Post, Tecplot or FieldView) convert this data into intuitive engineering visualisations such as:
Vector plots (velocity orientation fields).
Shaded contour plots (pressure and temperature distributions).
Particle tracking and streamline animations.
Quantitative data export for structural analysis codes (e.g., ABAQUS, ANSYS Mechanical) to study Fluid-Structure Interactions (FSI).

3.10 Advantages and Disadvantages

Advantages

- **Elimination of Linear Restrictions**: Capable of directly solving fully non-linear partial differential equations.
- **Complex Multi-Physics:** Simulates highly coupled phenomena such as chemical reactions, combustion, and radiative heat transfer.
- **High Resolution Data:** Provides exhaustive, full-field values for all relevant variables (p, u, T, k) across the entire spatial domain.
- **Rapid Design Iteration:** Allows engineers to rapidly screen hundreds of parametric design configurations without manufacturing physical prototypes.

Disadvantages

- **Numerical Errors:** Susceptible to round-off errors and spatial truncation errors from discretization schemes.
- **Boundary Dependency:** Solutions are highly sensitive to the accuracy of the user-prescribed boundary conditions.
- **Computational Cost:** High-fidelity simulations (such as DES or LES) require substantial high-performance computing (HPC) allocations and extensive execution time.

3.11 Applications of CFD

Aerospace and Defense: Predicting aircraft lift, parasitic drag, and wave-drag in supersonic regimes.

- **Marine Hydrodynamics:** Analyzing wave resistance, hull wakes, and propeller cavitation on maritime vessels.
- **Meteorology:** Large-scale atmospheric modeling and global weather forecasting**.**

3.12 Turbulence Modeling and Viscosity Prediction

To close the (RANS) equations, the (μ_t) must be predicted via empirical transport equations. Standard closure models include:

- one-equation model
- k-ε and k-ε models (2- models)
- k-ω (SST) model.

3.13 k-ε Model Framework

k-ε model describes phenomenon of synthesis, transport and annihilation of turbulent

kinetic energy. The total instantaneous kinetic energy (Ktot) of turbulent flow split into (K) & fluctuating (k)

$$K = \frac{1}{2}\left(U^2 + V^2 + W^2\right)$$

$$k = \frac{1}{2}\left(\overline{u'^2} + \overline{v'^2} + \overline{w'^2}\right)$$

$$k_{tot} = K + k$$

where ε = volumetric rate of viscous dissipation of turbulent kinetic energy given by turbulent dynamic eddy viscosity (μt) is modelled algebraically when both k and ε are known from empirical transport solutions:

$$\mu_t = \rho C_\mu \frac{k^2}{\varepsilon}$$

Where Cμ is a dimensionless empirical constant (typically equal to 0.09).

3.14 Exact Transport Equation for Turbulent Kinetic Energy (k)

In equation, tracking budget of k within a fluid flow is formulated as follows:

$$\frac{\partial(\rho k)}{\partial t} + \operatorname{div}(\rho k \mathbf{U}) = \operatorname{div}\left[-\overline{p'\mathbf{u}'} + 2\mu\overline{\mathbf{u}'e'_{ij}} - \frac{1}{2}\rho\overline{u'_i u'_i u'_j}\right]$$

$$- \rho\overline{u'_i u'_j} \cdot E_{ij} - 2\mu\overline{e'_{ij}e'_{ij}}$$

To understand the physical processes driving the turbulence energy budget, the terms can be systematically in the following manner

$$\underbrace{\frac{\partial(\rho k)}{\partial t}}_{\text{(1) Rate of Change}} + \underbrace{\operatorname{div}(\rho k \mathbf{U})}_{\text{(2) Convective Transport}} = \underbrace{\operatorname{div}\left(-\overline{p'\mathbf{u}'}\right)}_{\text{(3) Pressure Diffusion}} + \underbrace{\operatorname{div}\left(2\mu\overline{\mathbf{u}'e'_{ij}}\right)}_{\text{(4) Molecular Viscous Diffusion}} + \underbrace{\operatorname{div}\left(-\frac{1}{2}\rho\overline{u'_i u'_i u'_j}\right)}_{\text{(5) Turbulent Reynolds Diffusion}} + \underbrace{\left(-\rho\overline{u'_i u'_j} \cdot E_{ij}\right)}_{\text{(6) Shear Production } (P_k)} - \underbrace{2\mu\overline{e'_{ij}e'_{ij}}}_{\text{(7) Viscous Dissipation } (\rho\varepsilon)}$$

Where:

- E_{ij} represents mean rate-of-deformation tensor.
- e'_{ij} represents fluctuating component of rate of deformation
- Term (6) (P_k) represents transfer of kinetic energy from large-scale mean flow into turbulent fluctuations via Reynolds shear stresses.

Term (7) (ρε) represents the irreversible molecular destruction of turbulent energy into thermal internal energy via viscous shear forces at the Kolmogorov microscale.

3.15 Viscous Dissipation Rate

The viscous dissipation term in the k-transport equation is defined volumetrically as:

$$\rho\varepsilon = 2\mu\overline{e'_{ij}e'_{ij}}$$

This phrase matches the irreversible destruction rate of turbulent kinetic energy by the high-shear work done by the tiniest turbulent eddies (Kolmogorov microscale) against fluid viscous strains.

To estimate this tracking parameter independently of the local fluid density, the rate turbulent dissipation per unit mass (ε) is specified using,

kinematic viscosity (υ=μ / ρ) $\varepsilon = 2\nu\overline{e'_{ij}e'_{ij}}$

Where e'_{ij} = fluctuating component of rate-of-deformation. This explicit closure value supplies the destructive sink term of the typical two-equation k-ε

3.16 Turbulent dissipation (k -E):

Equations look quite similar.

"The k equation's reliance on primed quantities shows that turbulent interactions govern its variations

mostly controlled by turboulent interactions. Moreover, while term (7) appears identically in both budgets. its negative sign in the equation signifies destruction, whereas its positive sign in the equation represents production.

the direct transfer of kinetic energy from the mean flow into turbulence

$$K= -2\mu\overline{eij'eij'}$$

It describes dissipation of k because of work done by smallest eddies against the viscous stresses.

It defines, rate of dissipation/ unit mass ε as:

$$\varepsilon= 2\nu\overline{e_{ij}'e_{ij}'}$$

When comparing the transport budgets of (K) and tu (k), their respective mathematical equations exhibit a highly

symmetrical structural form. But they describe completely distinct physical interactions:

Decomposition of Scales: The k transport equation is mostly governed by primed (fluctuating) quantities. This shows that local variations of turbulent kinetic energy are driven only by non-linear turbulent-turbulent interactions

Energy Cascade Mechanism: The turbulence production term, term (7) in the previous section, exists in both energy budgets with opposite signs. It appears as a negative source (destruction) in the mean kinetic energy (K) equation,

and a positive source (creation) in turbulent kinetic energy (k) equation.

This mathematical opposition is a perfect image of the physical Reynolds energy cascade where the kinetic energy is removed from the large-scale mean flow and cascades down to the turbulent fluctuations.

CHAPTER 4

EXPERIMENTAL WORK

4.1 Analytical Flow Computations (Input Conditions)

The flow regime inside the proposed wind tunnel is strictly subsonic and low velocity such that compressibility effects can be neglected. Therefore, the fluid density (ρ) is constant and the steady, one-dimensional incompressible continuity equation is directly applicable are as following:

$$A1 * V1 = A2 * V2$$

Where,

A1 = Cross-sectional area at inlet of effuse (contraction nozzle) = 1.2 m2

A2 = Cross-sectional area at outlet of effuse (test section inlet) = 0.26 m2

V2 = Target freestream velocity inside the test chamber =16.2 m2

V1 = Required velocity at the effuse inlet

Unknown inlet velocity variable (V1)

$$V1=A2*V2/A1$$

$$V1=(0.26*16.2)/(1.2)$$

$$V1=3.51 \text{ m/sec}$$

This derived value V1 = 3.51 m/sec establishes the exact numerical

boundary condition for the velocity-inlet descriptor in the downstream simulation.

4.2 Ansys Workbench Simulation

1. ANSYS used to determine the simulations in Analysis System i.e. Fluid Flow
2. A dialoguee box opened in Project Schematic as given below
3. It is named as velocity eaternal 1.0

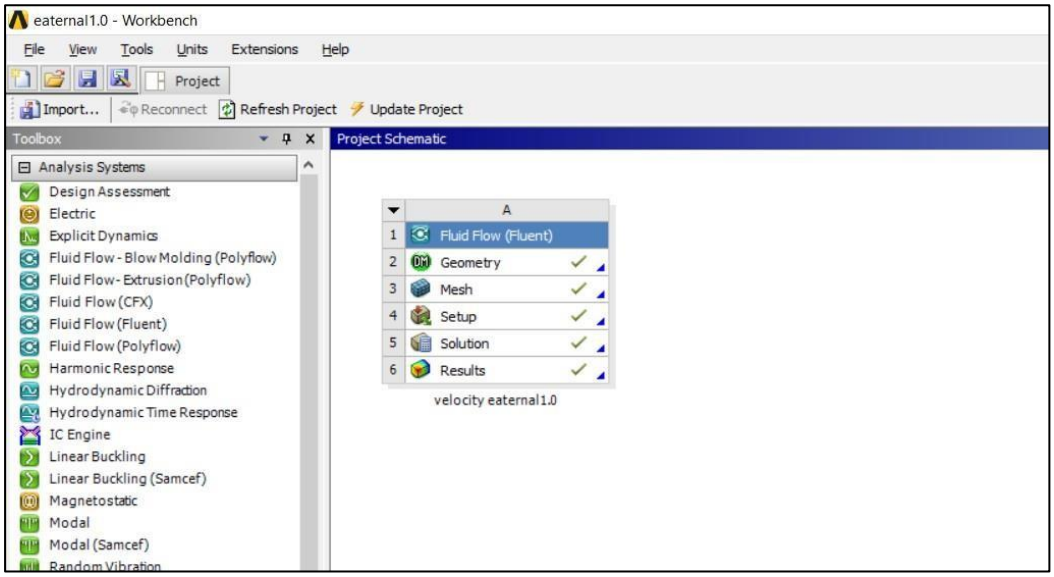

Figure 7: Ansys Dialogue Box

1. Geometry Generation and Preparation

The geometric model of the wind tunnel assembly was created in solid works and exported as an Initial Graphics Exchange Specification (.IGS) file. The import and clean-up pipeline in ANSYS Design Modeller was performed as follows:

1. **CAD Import:** Select Geometry ⟶ browse to locate and input the .IGS file, then click Import ⟶ generate to compile the solid bodies.
2. **Boolean Operations:** To isolate fluid domains and establish explicit interfaces, parts were differentiated or unified via:

   Create ⟶ Boolean ⟶ Operation Type ⟶ Named Selection
3. **Volume Extraction:** Internal gaps within the radiator assembly were extracted and sealed to isolate the internal fluid volume using:

   Tools ⟶ Fill ⟶ By Cavity / Named Selection

4. **Surface Repair:** Artifact faces generated during the CAD translation were cleaned and unified using:

   Tools ⟶ Merge ⟶ Face Selection

   Calculate baseline aerodynamic velocity fields prior to heat transfer mapping, the solid radiator matrices and water domains were suppressed, leaving only the primary air domain active.

2. Mesh Generation and Discretization

- The computational mesh was built with the ANSYS Meshing tool, to optimise the spatial resolution versus hardware limits:
- **Global Sizing Function:** The mesh sizing was set to Proximity and Curvature to accurately resolve high-curvature walls and thin fluid gaps.
- **Global Parameters:** Due to local hardware memory constraints, global options were set to a coarse relevance centre with medium smoothing. The specific cell size metrics were:
  - Minimum Proximity Size: 40mm
  - Maximum Face Size: 460mm
  - Maximum Element Size: 920mm
- **Local Refinement:** To resolve strong shear layers and velocity gradients inside the test chamber, a localized refinement pass was applied:

  Mesh ⟶ Insert ⟶ Refinement ⟶ Select Test Chamber Faces

  Boundary Labeling: The mesh finalized via Mesh ⟶ Generate Mesh. The boundaries were mapped into the solver using Named Selections to define the inlet, outlet, and wall surfaces.

3. Solver Setup and Physics Configuration

The discretised domain was imported to the ANSYS fluent solver in double precision mode on four parallel processors. The physics and boundary conditions were defined as:

- **General Settings**:

1. Solver Type: Pressure-Based
2. Velocity Formulation: Absolute
3. Time Dependence: Steady-State
4. Gravity: Enabled with an acceleration constant of g = 9.81 m/sec

- **Viscous Model:** The two-equation Realisable (k-ε) turbolence model was

findout,, together with Enhanced Wall Treatment (EWT) to provide stable boundary layer resolution near the solid walls.

- **Materials and Cell Zones:** The working fluid was replicated from the Fluent database as air with constant thermodynamic parameters and assigned globally under Cell Zone Conditions.
- **Boundary Conditions:**

Air Inlet: Set Velocity-Inlet with uniform crossectinal normal velocity of 3.51m/sec (derived from the upstream continuity equation calculations).

Air Outlet: Set Pressure-Outlet with a static gauge pressure of zero (atmospheric exhaust)

4.3 Recorded Data

Wind tunnel testing the most reliable approach to determine the distribution of wind pressure.

Typical procedure:

- Fabrication of scaled model
- Simulation of atmospheric boundary layer
- Pressure tap instrumentation
- Data acquisition and statistical analysis
- There are some key observations from the literature:
- Curvature reduces drag coefficient.
- Suction peaks are distributed rather than localized.
- Pressure variation increases with roof height

I have shown the recorded data and to create the contour profile as shown in figure below.

In this model having three faces (A, B & C)

Each face having total 49 taps points i.e. (7x7)

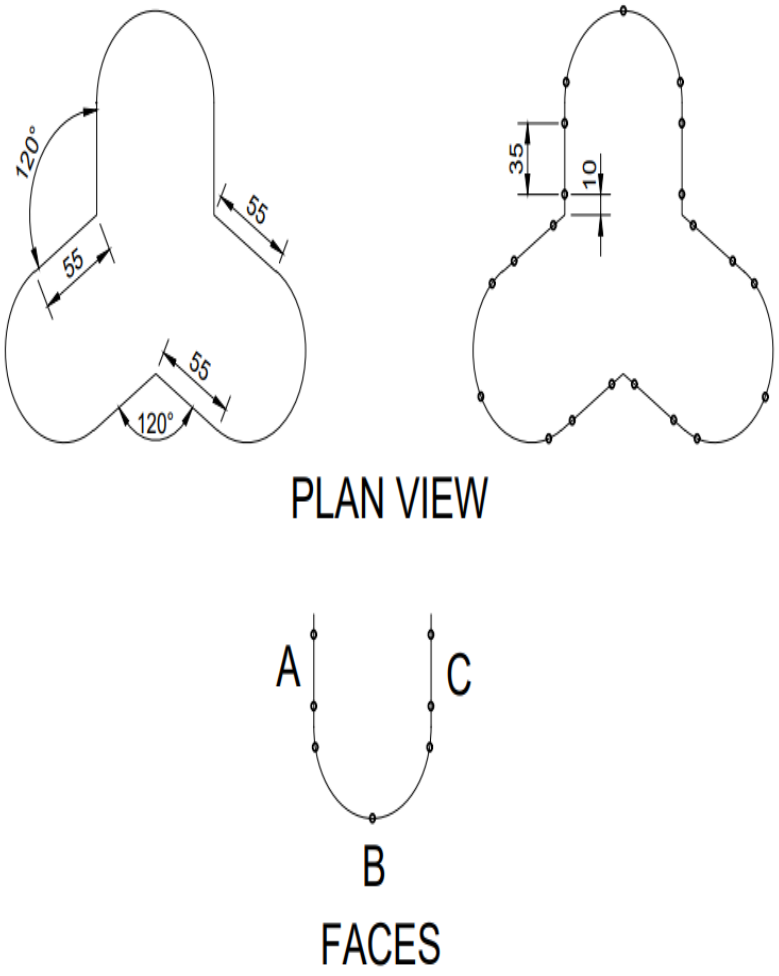

Figure 8: Model Plan View

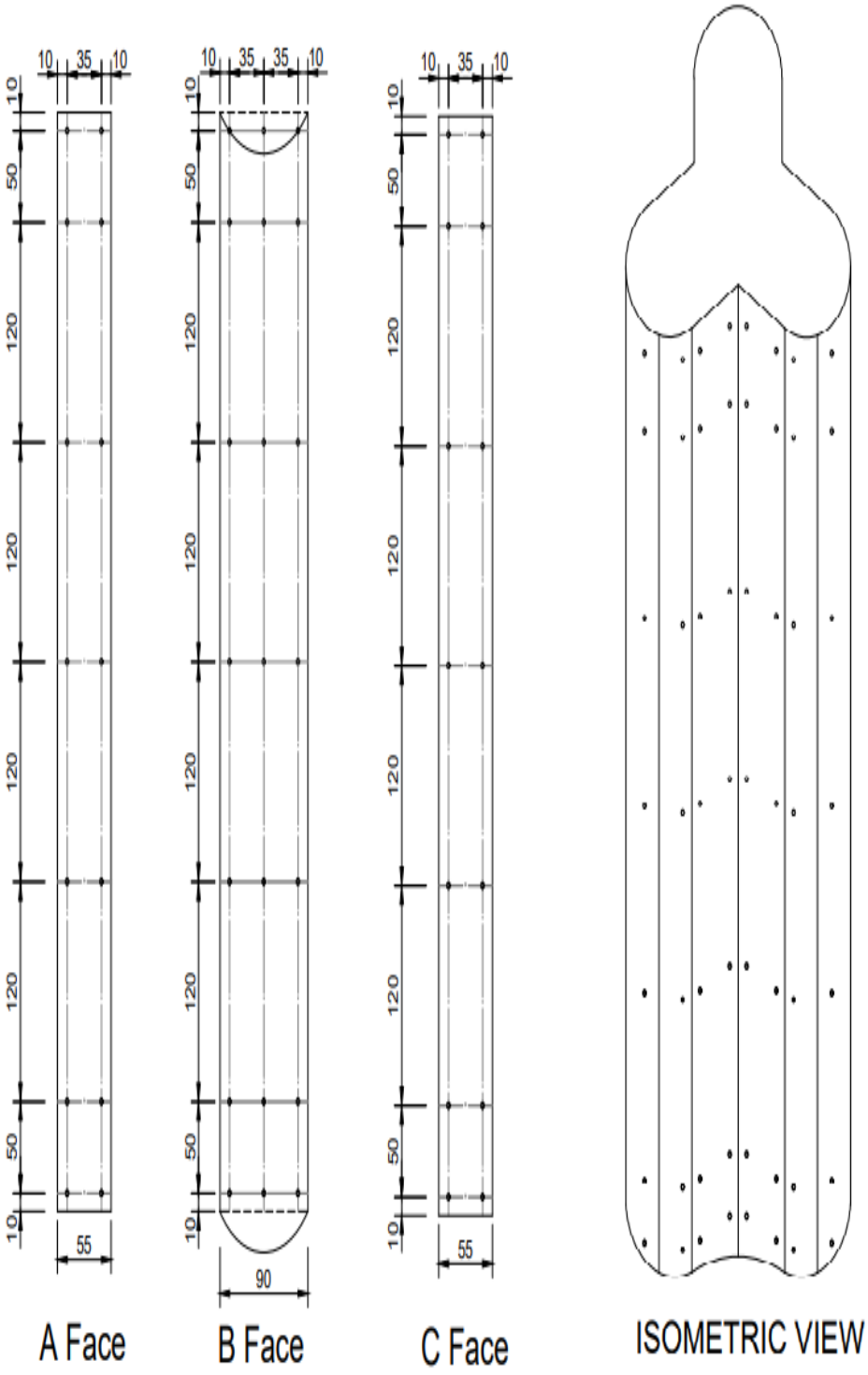

Figure 9: Model Elevation View

At Face A (0^0)

Max value of Cp	0.443333
Min value of Cp	-0.68333

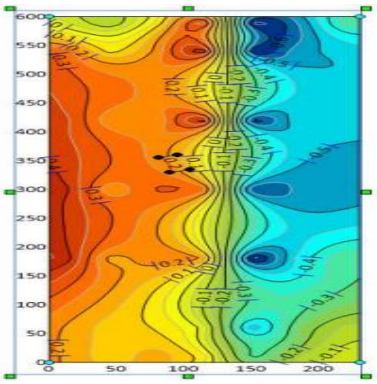

Figure 10:A (At 0^0)

At Face A (30^0)

Max value of Cp	0.67
Min value of Cp	-7.93333

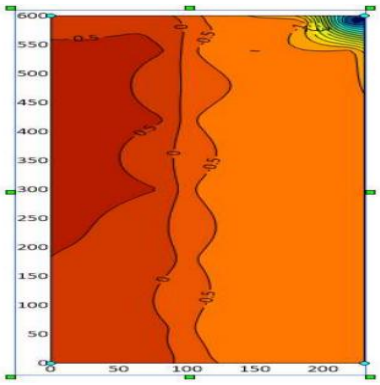

Figure 11: A *(*At 30^0)

At Face A (60^0)

Max value of Cp	0.603333
Min value of Cp	-0.885

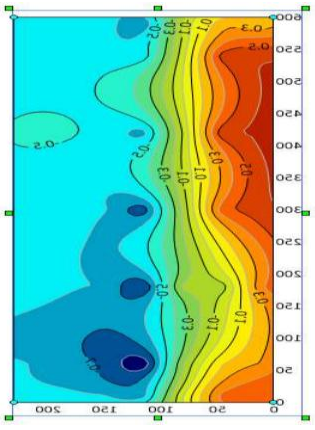

Figure 12-A (At 60^0)

At Face A (90^0)

Max value of Cp	0.498333
Min value of Cp	-0.86667

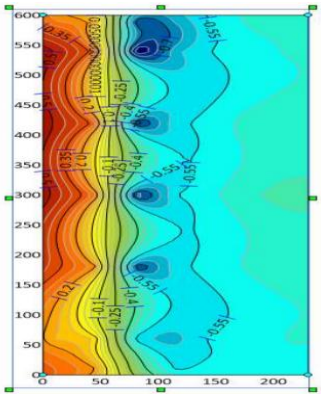

Figure 13-A (At 90^0)

At Face A (120^0)

Max value of Cp	0.071667
Min value of Cp	-1.24833

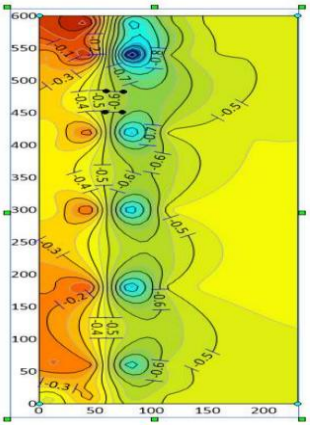

Figure 14: -A (At 120^0)

At Face A (150^0)

Max value of Cp	-0.388333333
Min value of Cp	-0.755

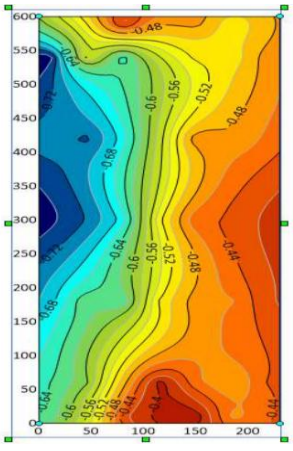

Figure 15:-A (At 150^0)

At Face A (180^0)

Max value of Cp	-0.44333
Min value of Cp	-0.73333

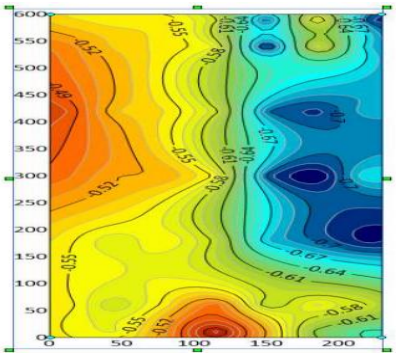

Figure 16: -A (At 180^0)

At Face B (0^0)

Max value of Cp	0.042
Min value of Cp	-1.37333

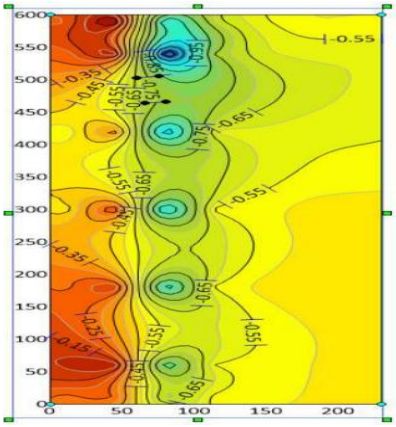

Figure 17: -B (At 0^0)

At Face B (30^0)

Max value of Cp	-0.31167
Min value of Cp	-0.78167

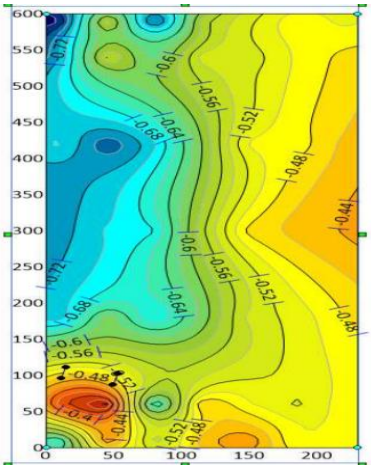

Figure 18: -B (At 30^0)

At Face B (60^0)

Max value of Cp	-0.385
Min value of Cp	-0.70333

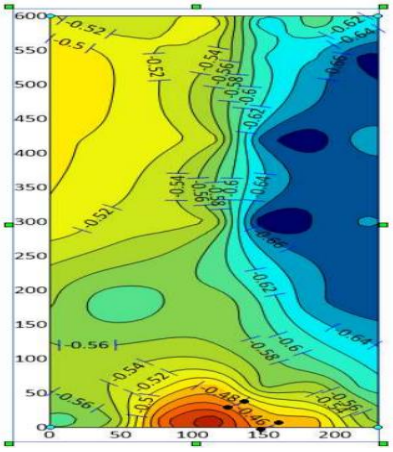

Figure 19: -B (At 60^0)

At Face B (90^0)

Max value of Cp	0.155
Min value of Cp	-1.12833

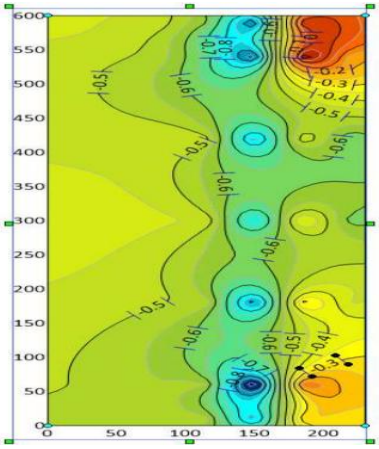

Figure 20: -B (At 90^0)

At Face B (120^0)

Max value of Cp	0.438333
Min value of Cp	-0.98667

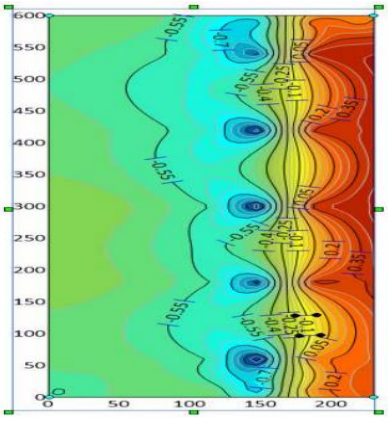

Figure 21: -B (At 120^0)

At Face B (150^0)

Max value of Cp	0.671667
Min value of Cp	-0.715

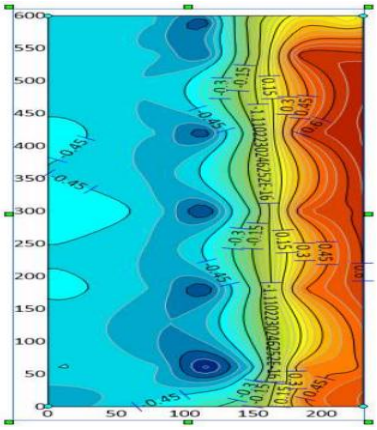

Figure 22: -B (At 150^0)

At Face B (180^0)

Max value of Cp	0.65
Min value of Cp	-1.015

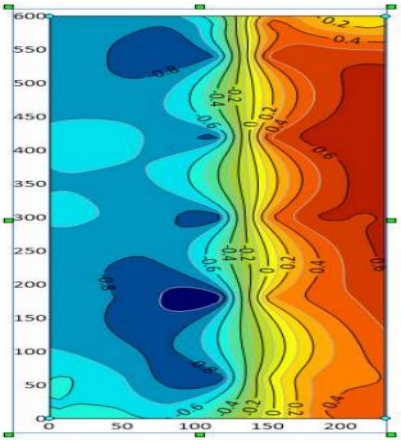

Figure 23: -B (At 180^0)

At Face C (0^0)

Max value of Cp	2.346667
Min value of Cp	-1.00833

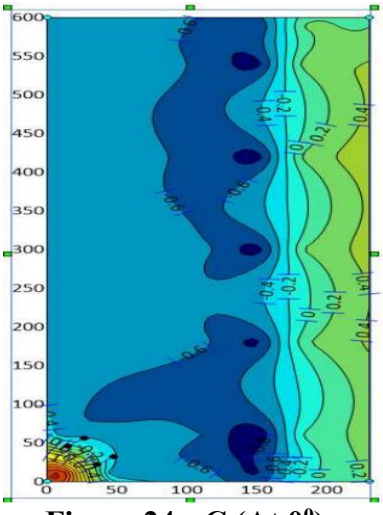

Figure 24: -C (At 0^0)

At Face C (30^0)

Max value of Cp	1.796667
Min value of Cp	-0.70667

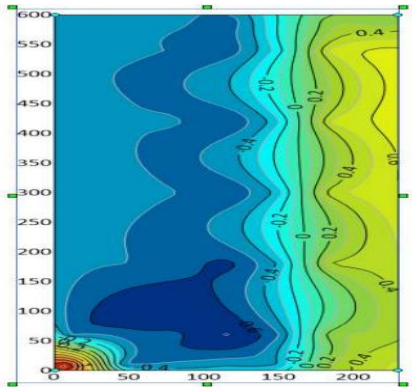

Figure 25: -C (At 30^0)

At Face C (60^0)

Max value of Cp	1.676667
Min value of Cp	-0.91667

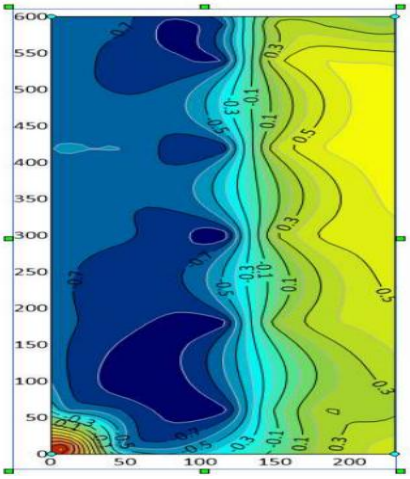

Figure 26: -C (At 60^0)

At Face C (90^0)

Max value of Cp	2.061667
Min value of Cp	-0.77333

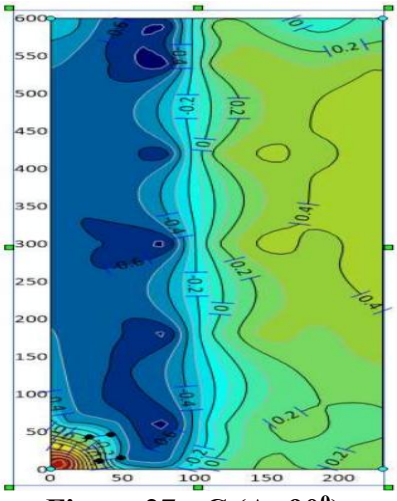

Figure 27: -C (At 90^0)

At Face C (120^0)

Max value of Cp	2.401667
Min value of Cp	-0.79167

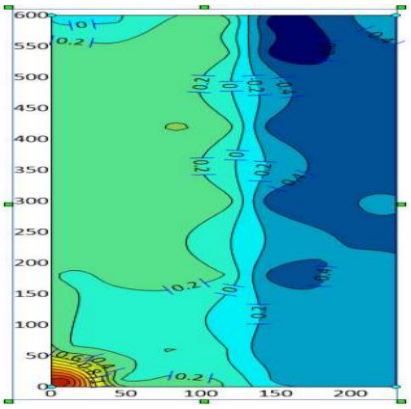

Figure 28: -C (At 120^0)

At Face C (150^0)

Max value of Cp	1.55
Min value of Cp	-1.08833

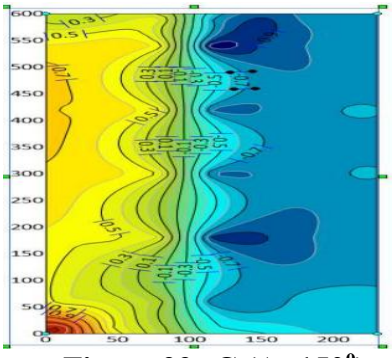

Figure 29:-C (At 150^0)

At Face C (180^0)

Max value of Cp	1.335
Min value of Cp	-0.81167

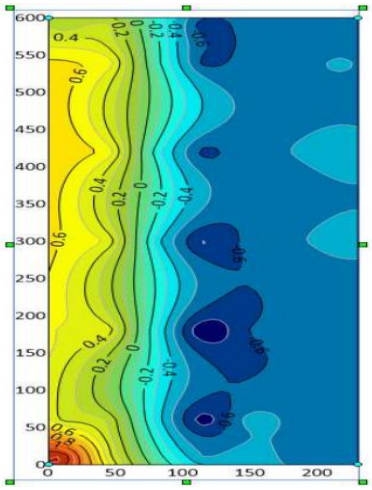

Figure 30:-C (At 180^0)

CHAPTER 5

RESULTS AND DISCUSSIONS

The mean pressure coefficient distribution showed positive pressures on the windward surface and high suction on the leeward and side surfaces. The effect of the curvature was to induce a more gradual change of pressure on the windward face, or a smoother flow attachment.

Especially at oblique wind angles and in the vicinity of the upper building levels near the flow separation zones strong fluctuating pressure coefficients were found. Such variations reflect increased unsteady flow effects that are important for cladding and façade design.

The highest suction pressures occurred for both normal and oblique wind directions showing the significance of multi-directional wind evaluations. Compared to normal rectangular buildings, the curved model resulted in a reduction of the global wind loads but an increase of localised suction pressures.

The results demonstrate that the curved geometries provide aerodynamic advantages, but also lead to critical localised loading conditions.

The post-processed velocity contours in the active fluid domain show a very regulated uniform distribution of flow. It is worth noting that the change of the velocity throughout the test section is quite small. This provides a consistent freestream flow field which is a very important pre-condition for accurate aerodynamic and thermal experiments.

The area weighted average function in ANSYS CFD-Post was used to evaluate the steady state velocity in the core of the test chamber:
V (Chamber), avg = 15.1 m/sec

This numerical result closely aligns with your target analytical design speed (15.1 m/sec), validating the geometric performance of your contraction nozzle (effuser) configuration.

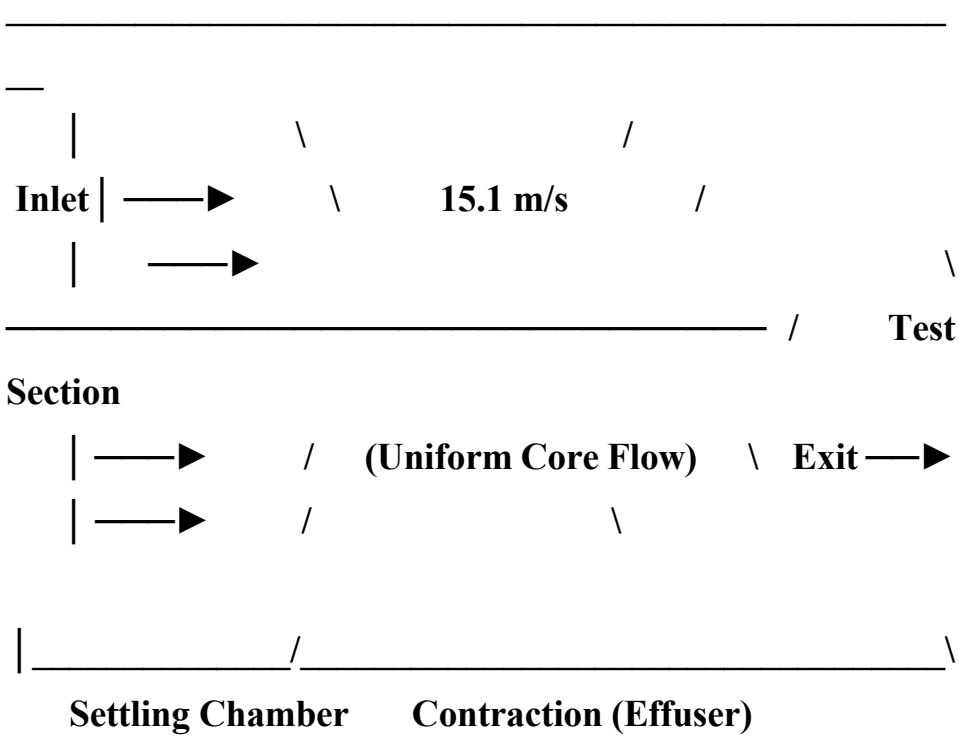

Figure 1. Diagram of acceleration across the contraction section.

CHAPTER 6

CONCLUSION

In this experiment, the curved-shaped high-rise buildings are greatly influencing the calculation of wind pressure. The curvature is able to minimise the overall aerodynamic drag. It however protrudes into localised regions of high negative pressure and greater pressure variations.

The pressure measurements at each tap are transformed to a dimensionless metric termed the pressure coefficient Cp.

Critical wind effects were identified under oblique wind directions, and a thorough directional analysis is required. The high-rise constructions require wind tunnel testing since the normal code requirements may not correctly reflect the complicated pressure patterns.

The experiment investigation showed that the curved-shaped high-rise structures change the wind pressure distribution greatly compared with the traditional forms. The curvature reduces the overall aerodynamic drag but generates local high-pressure variations and high negative pressure zones. Critical wind loads were identified for oblique wind directions, and a full directional analysis is required.

Wind tunnel testing is important for curved high-rise structures because the complicated pattern of pressure distributions may not be adequately predicted by typical code standards. The results give important data for safe structural and façade design of curved tall buildings.

REFERENCES

[1] *Assainar N, Dalui SK. Aerodynamic analysis of pentagon-shaped tall buildings. Asian J Cin Eng. 2021;22:33-48*

[2] *American Society of Civil Engineers. Minimum design loads and associated criteria for buildings and other structures (ASCE/SEI 7-16). Reston, VA: ASCE, 2016. https://doi.org/10.1061/9780784414248*

[3] *American Society of Civil Engineers. Minimum design loads and associated criteria for buildings and other structures (ASCE/SEI 7-16). Reston, VA: ASCE, 2016. https://doi.org/10.1061/9780784414248*

[4] *Baskaran A. Wind engineering studies on tall buildings transition in research, building and environment. Build Environ. 1993;28(1):1-19.*

[5] *Bandi EK, Tamura Y, Yoshida A, Kim YC, Yang Q. Experimental investigation on aerodynamic characteristics of various triangular-section high-rise buildings. J Wind Eng Ind Aerod. 2013;122:60-68. https://doi.org/10.1016/j.jweia.2013.07.002*

[6] *Beneke DL, Kwok KCS. Aerodynamic effect of wind induced torsion on tall buildings. J Wind Eng Ind Aerod. 1993;50:271-280. https://doi.org/10.1016/0167-6105(93)90082-Y*

[7] *Bhattacharyya B, Dalui SK. Investigation of mean wind pressures on 'E' plan shaped tall building. Wind Struct Int J. 2018;.*

[8] *Bairagi AK, Dalui SK. Wind environment around the setback building models. Build Simul. 2021;14:1525- 1541.*

[9] *Chaurasia AK, Anand AK, Meena A, Sharma D, Raj R. CFD simulation of wind-induced interference effects on low-rise gable roof structure using ANSYS. Eng Res Trans. 2024;7:63-74. https://doi.org/10.55084/grinrey/ERT/978-81-964105- 4-4*

[10] *Cheung JCK, Melbourne WH. Torsional moments of tall buildings. J Wind Eng Ind Aerod. 1992;42(1- 3):1125-1126. https://doi.org/10.1016/0167-6105(92)90119-U*

[11] *Cui DJ, Mak CM, Kwok KCS, Ai ZT. CFD simulation of the effect*

of an upstream building on the inter-unit dispersion in a multi-story building in two wind directions. J Wind Eng Ind Aerodyn.

[12] *Chauhan BS, Ahuja AK. Height effect of interfering buildings on wind pressure distribution on rectangular plan tall buildings.*

[13] *Shivashaankar DS, Yashwant PR. Earthquake resistant high rise buildings new concept. Int J Adv Res Eng Technol. 2014;5(6):121-124.*

[14] *Dogan T, Kastner P. Streamlined CFD simulation framework to generate wind-pressure coefficients on building facades for airflow network simulations. Build Simul.*

[15] *Gaur N, Raj R. Aerodynamic mitigation by corner modification on square model under wind loads employing CFD and wind tunnel. Ain Shams Eng J, 2021.*

[16] *Guedes P (Ed). Encyclopedia of Architectural Technology. McGraw-Hill, Gaylord EH, Gaylord CN. Structural Engineering Handbook, 1979.*

[17] *Yadav H, Roy AK. Wind induced aerodynamics responses of triangular high-rise buildings with varying cross-section areas. Asian J Civ Eng, 2024.*

PLAGIARISM REPORT

Experimental Study on the effect of Wind Pressure Disrubution on a Curved Shape Structure

ORIGINALITY REPORT

9%	7%	3%	4%
SIMILARITY INDEX	INTERNET SOURCES	PUBLICATIONS	STUDENT PAPERS

PRIMARY SOURCES

1	mechanical.anits.edu.in Internet Source	3%
2	archive.org Internet Source	1%
3	nmbu.brage.unit.no Internet Source	<1%
4	kipdf.com Internet Source	<1%
5	Submitted to University of Petroleum and Energy Studies Student Paper	<1%
6	Submitted to University of Leeds Student Paper	<1%
7	ebin.pub Internet Source	<1%
8	Submitted to Jawaharlal Nehru Technological University Student Paper	<1%